DOI 10.24425/aee.2022.142121

Development and performance analysis of a novel multiphase doubly-fed induction generator

ROLAND RYNDZIONEK, KRZYSZTOF BLECHARZ, FILIP KUTT, MICHAŁ MICHNA ✉, GRZEGORZ KOSTRO

Gdansk University of Technology
Faculty of Electrical and Control Engineering
Gabriela Narutowicza str. 11/12, 80-233 Gdańsk, Poland

e-mail: {roland.ryndzionek/krzysztof.blecharz/filip.kutt/✉michal.michna/grzegorz.kostro}@pg.edu.pl

(Received: 03.06.2022, revised: 13.07.2022)

Abstract: This paper presents the research into the design and performance analysis of a novel five-phase doubly-fed induction generator (DFIG). The designed DFIG is developed based on standard induction motor components and equipped with a five-phase rotor winding supplied from the five-phase inverter. This approach allows the machine to be both efficient and reliable due to the ability of the five-phase rotor winding to operate during single or dual-phase failure. The paper presents the newly designed DFIG validation and verification based on the finite element analysis (FEA) and laboratory tests.

Key words: doubly-fed induction generator, induction generator, multiphase machine, wind power generation

1. Introduction

Modern distributed power generation systems are designed based on safe and reliable operation. Following this approach, distributed wind generation systems are designed to operate at low voltage and under on and off-grid conditions.

Various electrical machines are used as electromechanical power converters or generators. The most commonly used types in wind power plants are: the direct driven permanent magnet generator (PMG), electromagnetically excited synchronous generator (SG), and doubly-fed induction generator (DFIG) [1–5]. All of those machines have their advantages and disadvantages. The PMG is reasonably reliable and can operate at variable speeds. However, the induced electromotive force (EMF) cannot be removed entirely due to the lack of excitation control. For the

variable speed operation, an inverter is required. In addition, the uncertainty regarding rare earth metals is a critical limiting factor for this technology [6].

The electromagnetically excited synchronous generator, unlike the PMG has a controllable excitation flux, which increases the safety of operation. However, the variable speed operation also requires an inverter. The slip rings and brushes assembly can be replaced with a brushless exciter, reducing the maintenance requirement and increasing the generator's complexity [7].

One machine designed to mitigate the main drawbacks mentioned above is the DFIG. This generator allows for variable speed operation. Even though the converter is still required, it is only responsible for converting part of the over-generation power [8,9]. The main disadvantages of such a system are the slip contact between slip rings and brushes and the reliability of the rotor side (RSC) or grid side (GSC) converters [10,11]. The principle of operation of this system is based on an induction generator where stator windings are connected directly to the grid and rotor windings are supplied by a bidirectional power converter (Fig. 1).

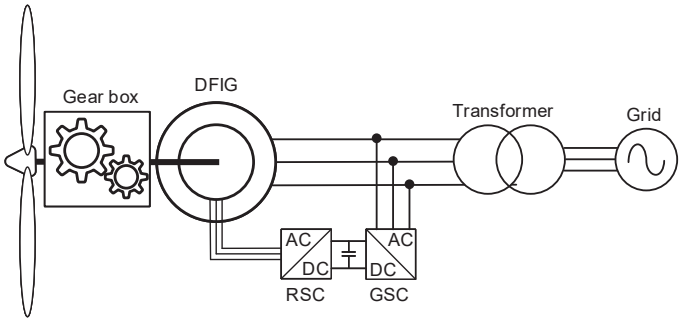

Fig. 1. The typical configuration DFIG wind turbine system

The wear and tear of the slip ring assembly is the factor that discourage investors. This issue can be solved by eliminating the slip ring assembly and using a brushless doubly-fed induction generator [12]. However, this solution also has its drawbacks, such as the requirement for 3 machine windings, two on the stator and one on the rotor, and the need for both RSC and GSC converters. Even though the slip ring assembly is eliminated still, the failure of only one phase branch of the three-phase power converter would render the machine unusable.

This paper develops a design process for a distributed power generation system for a multiphase double-fed induction generator (Fig. 2). The designed DFIG is equipped with a five-phase rotor winding supplied from the five-phase inverter. The proposed solution of the novel five-phase rotor DFIG allows for fault-tolerant operation by maintaining the possibility of creating a rotating magnetic field by the rotor winding in the case of a single or dual rotor failure.

The modern wind power generation system requires a generator that can supply both active and reactive power. In addition, distributed power generation requires the generation system to operate under overexcited conditions. For this purpose, the machine is built based on an induction motor's standard stator core and winding. To facilitate the operation with higher than the nominal EMF of the generator node, the stator winding is designed to operate in both star and delta configurations allowing for more flexible voltage and reactive power control [13].

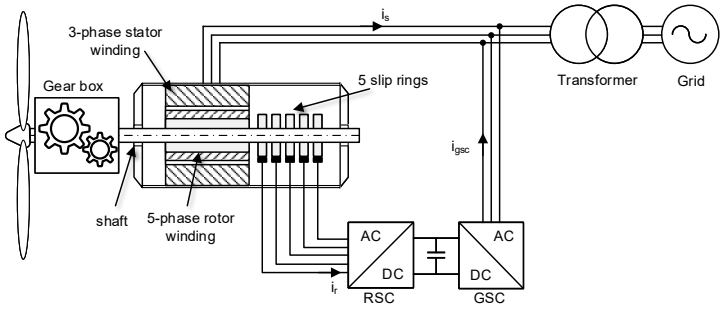

Fig. 2. The new configuration of a multiphase DFIG wind turbine system

2. Objective and scope

This research aims to demonstrate the validity of the doubly-fed induction generator construction design based on a standard induction motor stator.

This paper is organized as follows. Section 3 offers the description of the design process and the main parameters of the developed prototype. Section 4 presents the finite element model development to validate the designed machine. The measurements performed on the prototype are compared with the finite element analysis (FEA) simulations in section 5, allowing for the verification of the design approach. Section 6 concludes the validity of the proposed approach.

The main contributions of the presented research are:

– Development of a novel multiphase doubly-fed induction generator based on the standard induction motor stator.
– Design prototype verification using both FEA simulations and measurement implementation of the generator operating in off-grid conditions.
– The generation system with the five-phase inverter that supplies the rotor winding under no-load, active and reactive load conditions.
– Demonstrated fault-tolerant operation in the off-grid power generation system.

3. Generator design

The proposed research prototype was developed based on components of a typical induction machine. The entire stator assembly and the enclosure of the induction machine were reused. This was done for two reasons. It allowed the prototype to be built quickly. Using a stator in both star and delta configurations allowed the machine to operate in overexcited conditions without significant core saturation. The essence of the project was the appropriate design of the rotor with a 5-phase slip-ring winding. The main assumption was that the rotor should have a similar number of turns per phase as the stator winding. The main concern was the maximum operating voltage of the RSC and GSC connecting the rotor to the grid. This was done so that in the case of machine sizing rotation, the rotor voltage would not be greater than the grid voltage while operating in on-grid conditions.

The proposed DFIG was designed to operate at rotation velocities from 0.7 to 1.3 times the synchronous speed. That meant about 30% of the generated power would have to be drawn from or supplied to the rotor winding. In addition, the required machine magnetization reactive power should be supplied from the rotor side of the machine. However, operating in star configuration @400V, the nominal power of the generator is decreased to 4 kW of electrical output power.

The main parameters of the designed DFIG are presented in Table 1. The view of the designed enclosure extension and rotor with the slip ring assembly is shown in Fig. 3.

Table 1. Main specification of the five phase DFIG

Parameter	**Value**
Rated power	4 kW
Voltage	400 V
Speed	1 000 rpm
Pair poles	3
Stator phases	3
Rotor phases	5
Stator external diameter	208 mm
Rotor external diameter	147 mm
Rotor core length	157 mm
Number of stator slots	36
Number of rotor slots	30
Number of pole pairs	3
Number of stator phases	3
Number of rotor phases	5
Number of rotor slots per pole and per phase	1
Air gap length	0.3 mm
Skewing of rotor	1 slot pitch
Number of winding layers	1 (single)

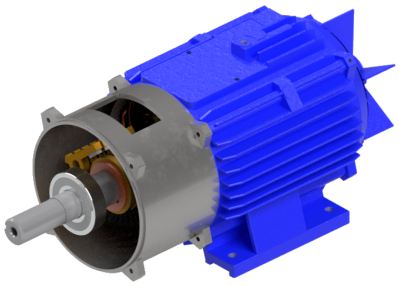

Fig. 3. The 3D virtual model of the novel 5-phase DFIG

4. Finite element model development

The proposed DFIG design was verified using finite element method (FEM) simulations in Ansys Maxwell software and the RMxpert Design tool [14]. The FEA validated the prototype's capability to perform under different operating conditions. The RMxpert module in Ansys Maxwell software was used to generate a geometrical model based on machine design requirements and to perform analytical calculations. Ansys Maxwell software was used to define the material attributes, boundary conditions, and the motor's moving parts for the FEM simulations; Fig. 4 shows the geometry of the model.

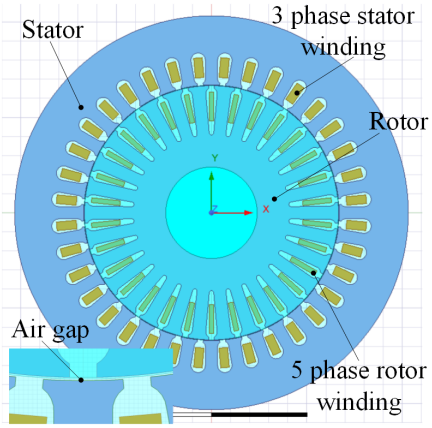

Fig. 4. Two-dimensional model of DFIG

The air gap magnetic flux density B_δ can be directly defined by the required value based on the design of the machine or can be calculated from the mmf curve as

$$B\delta(\alpha) = \mu_0 H_\delta(\alpha) = \mu_0 \cdot \frac{F_{m\delta}(\alpha)}{k_c \delta} = \mu_0 \cdot \frac{F_m(\alpha)}{k_F K_c \delta}, \tag{1}$$

where: α is the angular position at the periphery of the machine, μ_0 is the permeability of the vacuum, H_δ is the air gap magnetic field strength, F_m is the magnetomotive force, k_c is the Carter factor, δ is the air gap length, k_F is the magnetic circuit saturation ratio.

The entire model is used to build geometry, and its total number of mesh elements is roughly 12 000. The results are almost the same as for the model with 20 000 elements. The time step in the transient simulation was 0.2 ms, and the save fields were 2 ms. During the FEA, the rotor winding was excited by a 5-phase voltage source using a developed external circuit model. The simulations have been performed for the generator operation in off-grid conditions with a resistive load connected to the stator terminals. Both the on-load and off-load tests have been conducted. Figure 5(a) shows the 2D FEM simulation of DFIG's flux density distribution. The RMS (root mean square) rotor current value is around 1.5 A, and the level of the maximum flux density in the rotor slot is 1.2 T. The maximum value of flux density in the air gap is 0.75 T (Fig. 5(b)). The results also show that the flux distribution in a 2D environment exhibits the stator and rotor slot distribution (no skewing is implemented in the 2D FEM model).

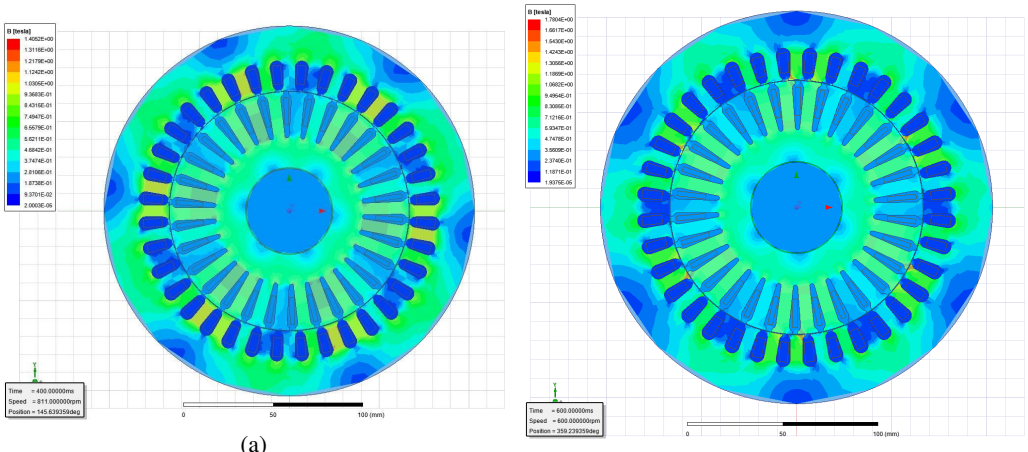

(a) (b)

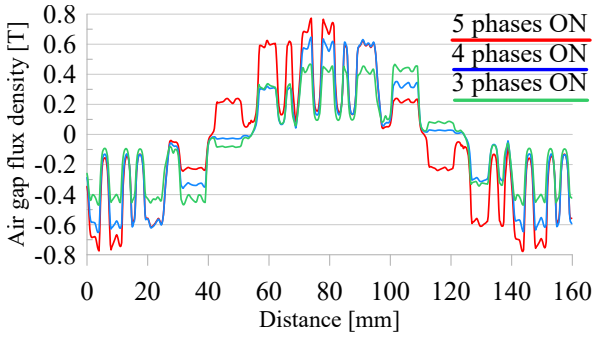

(c)

Fig. 5. The FEA simulation of the flux density distribution in stator and rotor core under no-load conditions (a); the FEA simulation of the flux density distribution in stator and rotor core under resistive load conditions (b); the air-gap magnetic flux distribution with 5 phases ON and fault winding cases (c)

The fault-tolerant performance has been prepared. The faulty operation conditions with one rotor phase failure have been simulated. The comparison is presented in Fig. 5(c). It could be noticed that with only 4 or even 3 rotor phases working (ON), the average magnetic field is smaller than with all 5 rotor phases working (ON), and as could be seen in some rotor teeth, the magnetic field is negligible.

Figure 5(b) presents the flux distributions under the resistive active load conditions. The RMS rotor current value is around 4.4 A. The maximum flux density value in the rotor teeth is around 1.5 T. The maximum value of flux density in the air gap is about 1 T. All results fit in desired ranges and meet the requirements.

Finally, the simulation results and laboratory measurements have been compared in the next section dedicated to prototype performance measurements.

5. Design verification

Developed prototype measurements have been performed to verify the results of the FEA. The measurements were performed during both no-load and load off-grid operation of the developed DFIG. The five-phase rotor winding was supplied from a five-phase voltage inverter. In contrast, the stator winding was connected to a variable symmetric three-phase load. This connection corresponds to the configuration of the generator operating in the standalone mode (Fig. 6(a)). Five-phase voltage inverter allowed for smooth rotor voltage amplitude and frequency adjustment. Used during the measurements two-level voltage inverter is a structure entirely developed at the Gdansk University of Technology. Such inverters are also used for supplying five-phase induction motors developed at the university.

The laboratory test bench was constructed using a designed five-phase DFIG driven by the 5.5 kW induction motor (Fig. 6(b)). The prime mover induction motor is supplied from its own inverter for accurate rotational velocity control. The 5.5 kW induction motor is mechanically coupled with a five-phases DFIG. This drive system configuration enables the generator rotational speed regulation in a wide range.

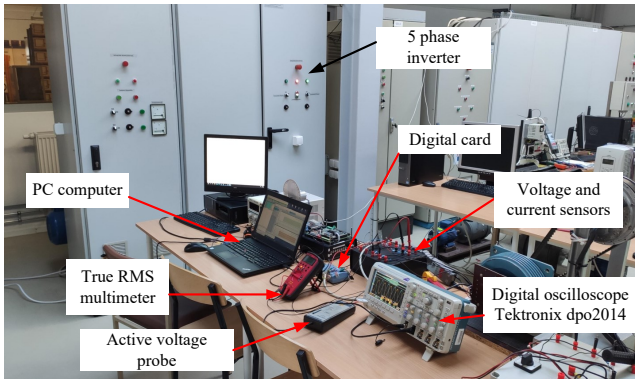

(a)

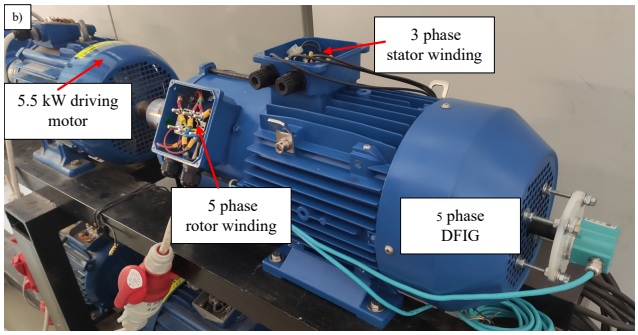

(b)

Fig. 6. The laboratory test bench of the five-phase DFIG prototype (a); the prototype five-phase DFIG (b)

The first measurement was performed at a speed of 810 rpm without any load. The DFIG stator is star-connected. The measurements have been made for different rotor currents and have been compared with simulation results.

Figure 7 shows the experimental test results. The rotor current exciting the machine is raised several times over the measurement period. These results have been compared with the FEA simulations (with the third and fourth/final steps in the rotor current rising sequence). Figure 8

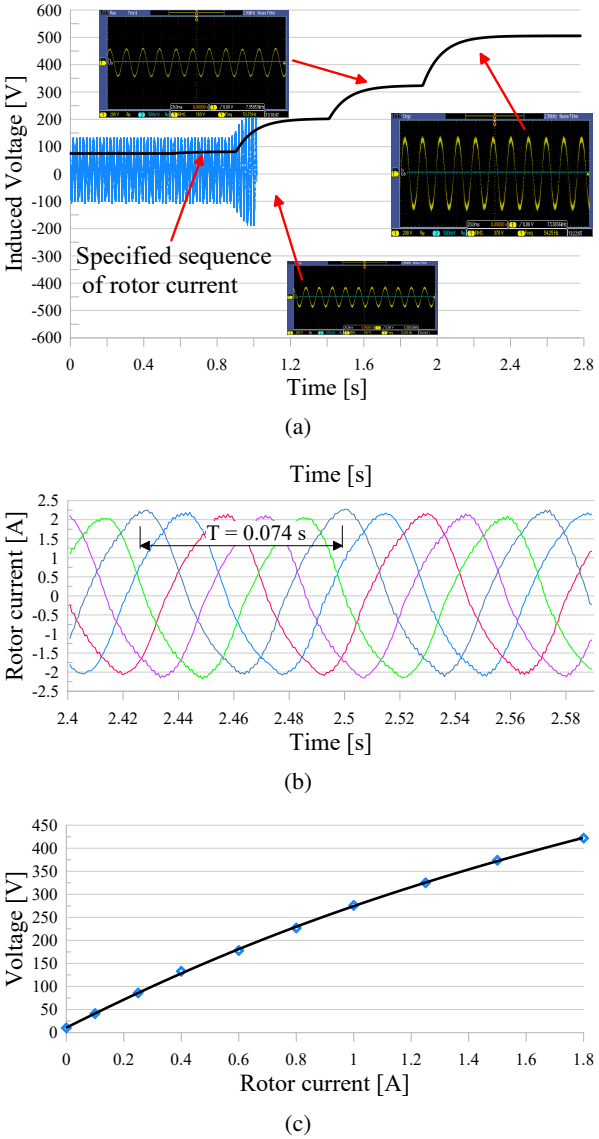

Fig. 7. No-load experimental tests: the induced voltage V_{l-l} (a); the five-phase rotor current waveforms, Ir RMS = 1.5 A (b); the open-circuit characteristic (c)

presents the comparison between the measurements and simulation results. The waveforms show good convergence between the simulations and measurements, around 10–15 V at amplitude.

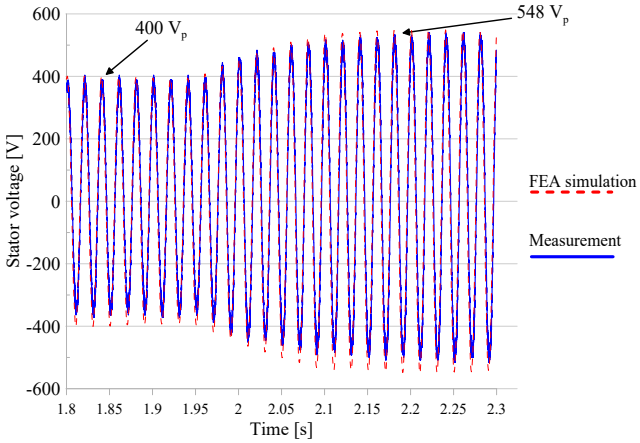

Fig. 8. Induced voltage measurement and simulation under the different rotor excitation current levels (Ir RMS = 1.5 A)

The load test has been performed. Firstly, the resistive load has been applied, and secondly, a mix of resistive and inductive loads has been used.

Figure 9 presents the laboratory test under the resistive load – 23 Ω. To achieve higher voltage, the rotor excitation current has been increased. Under the load, approx. 2 kW, the voltage and

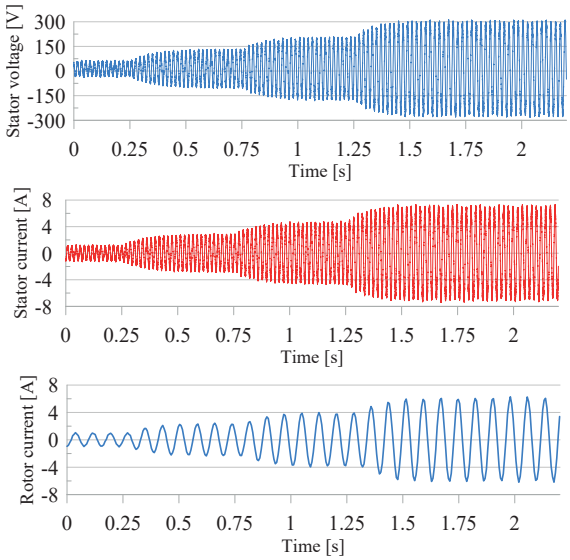

Fig. 9. Resistive load (23 Ω) experimental test with different rotor current excitation sequences – stator voltage, stator current, and rotor current waveforms

current maintained sinusoidal and 50 Hz. Moreover, the harmonic spectrum analysis shows a total harmonic distortion (THD) value of less than 2% for different load cases.

The laboratory measurements and FEM simulation results have been compared (Fig. 10). The results show good convergence of the reported results.

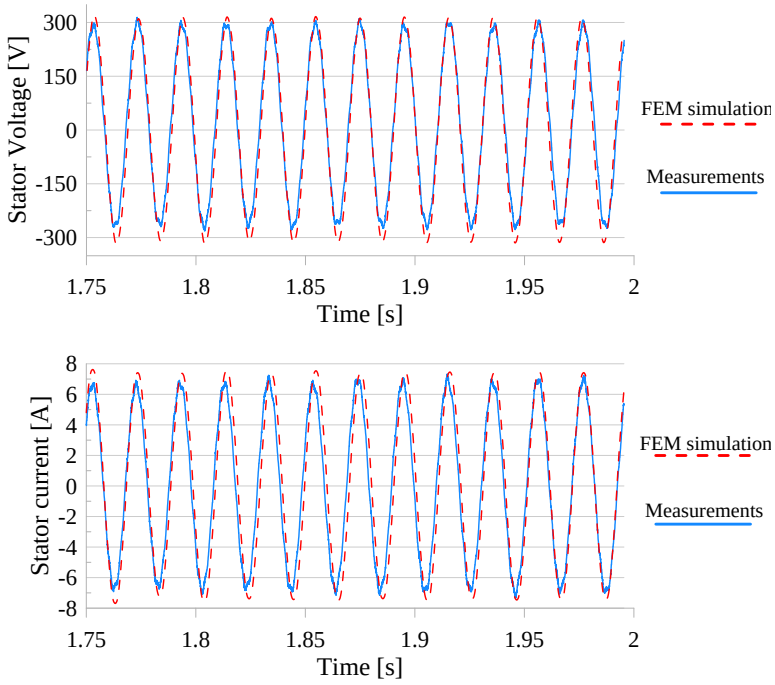

Fig. 10. The experimental and FEM simulation results under the resistive load

In Fig. 11, the mixed load test has been performed. The active and reactive power was approx. 2 kW and 0.5 kVar.

Finally, the fault-tolerant performance of the proposed five-phase DFIG was analyzed. Firstly, the no-load test has been performed. Secondly, the tests with different electric load levels were conducted. The single and dual rotor phase failures (disconnections) have been applied to the machine during its operation. The performed measurements were conducted during rotor phase A (first) and/or C (third) disconnection.

In Fig. 12, rotor phase A is briefly disconnected during the machine operation under no-load conditions (phase A – ON, phase A – OFF, phase A – ON sequence). As could be noticed, the stator voltage drops approx. 20 V. Although the one-rotor phase is disconnected, the stator voltage waveform shape is not affected. However, a slight asymmetry in the stator three-phase system could be noticed. The measured stator RMS voltages on each phase differ by about 5–8 V.

During the load conditions (Fig. 13(a)), a single-rotor phase failure also causes a decrease in amplitude and an asymmetry in stator voltage. The dual-rotor failure exacerbates this even further. However, because the voltage is still generated, the excitation five-phase converter algorithm can be developed to mitigate the changes in amplitude and shape of the air-gap flux distribution

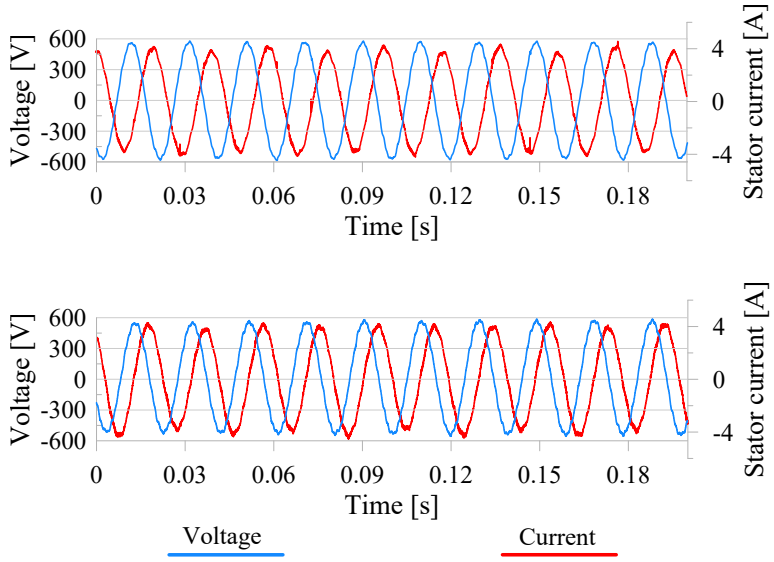

Fig. 11. The laboratory test under the resistive and inductive loads

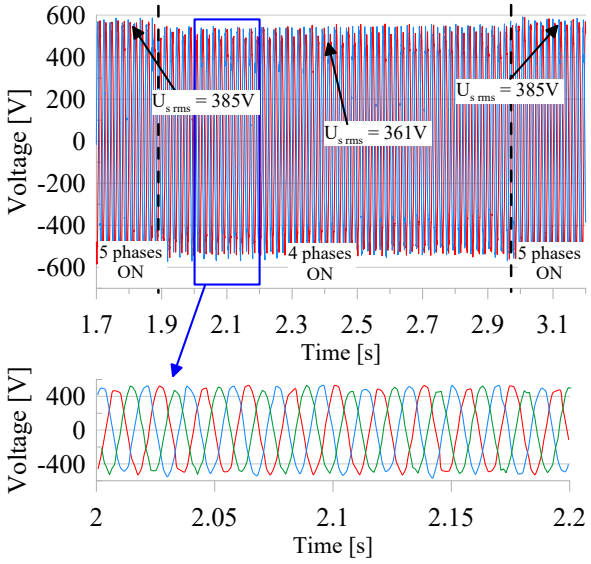

Fig. 12. The laboratory test of one rotor phase failure – no-load test

for adequate fault-tolerant performance. Moreover, the same tendency could be noticed in stator currents (Fig. 13(b)). The asymmetry appears under the rotor failure; however, the stator current is still sinusoidal. The active power in a single and dual-rotor failure decreases by 20% and 50%, respectively.

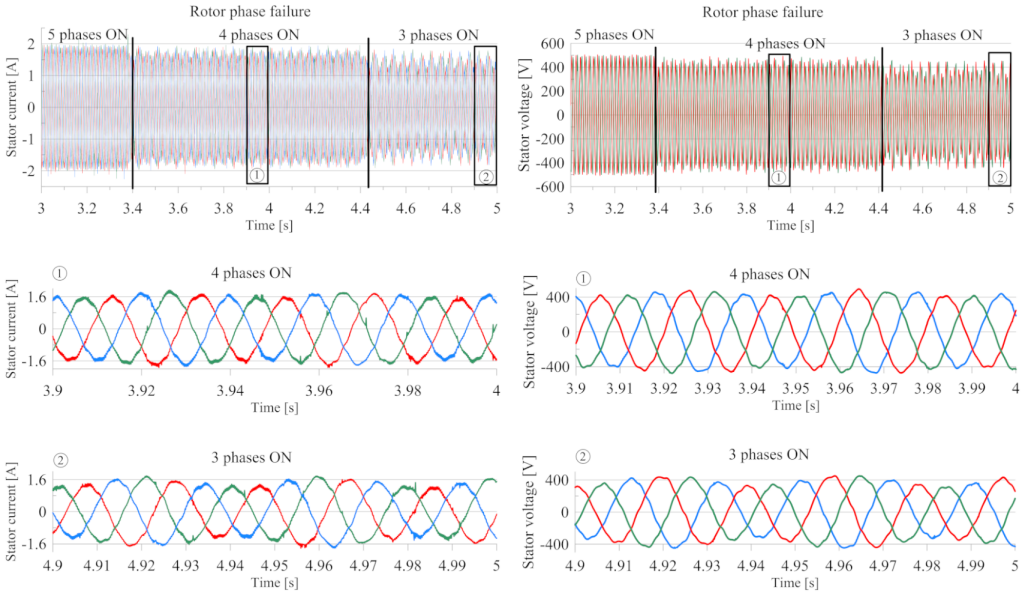

Fig. 13. The laboratory test of one-rotor phase failure – load test

The obtained reliability test results are far more than acceptable to state that the proposed approach allows for the generation system fault-tolerant performance concerning a single or dual-phase failure of the rotor winding.

6. Conclusions

The developed prototype was designed and investigated during the design process. Assumptions and calculations have been verified by FEA and measurements performed on the prototype. The DFIG with a five-phase rotor can operate as a regular three-phase machine in an electric power generation system. However, the main advantage of the designed machine is its fault-tolerant operation capabilities, mitigating one of the drawbacks of inverter-fed DFIG generation systems. Further investigation into the machine performance will focus on coping with output power quality during single or even dual-rotor phase failures due to the inverter or slip ring assembly fault. The proposed construction should be optimized, and a dedicated stator for the DFIG should also be developed in future research. However, even with the standard motor stator, the machine could supply the load with both active and reactive power.

The generator design is currently subject to a patent procedure by the Patent Office of the Republic of Poland (No. P.437248).

References

[1] Patil N.S., Bhosle Y.N., *A review on wind turbine generator topologies*, International Conference on Power, Energy and Control (ICPEC), Dindigul, India, pp. 625–629 (2013), DOI: 10.1109/ICPEC.2013.6527733.

[2] Zhang Y., Ula S., *Comparison and evaluation of three main types of wind turbines*, 2008 IEEE/PES Transmission and Distribution Conference and Exposition, Chicago, IL, USA, pp. 1–6 (2008), DOI: 10.1109/TDC.2008.4517282.

[3] Beainy A., Maatouk C., Moubayed N., Kaddah F., *Comparison of different types of generator for wind energy conversion system topologies*, 3rd International Conference on Renewable Energies for Developing Countries (REDEC), Zouk Mosbeh, Lebanon, pp. 1–6 (2016), DOI: 10.1109/REDEC.2016.7577535.

[4] Gupta R.A., Singh B., Jain B.B., *Wind energy conversion system using PMSG*, 2015 International Conference on Recent Developments in Control, Automation and Power Engineering (RDCAPE), Noida, India, pp. 199–203 (2015), DOI: 10.1109/RDCAPE.2015.7281395.

[5] Su M., Dong H., Liu K., Zou W., *Subsynchronous oscillation and its mitigation of VSC-MTDC with doubly-fed induction generator-based wind farm integration*, Archives of Electrical Engineering, vol. 70, no. 1, pp. 53–72 (2021), DOI: 10.24425/aee.2021.136052.

[6] McKenna R., Ostman P., Leye V.D., Fichtner W., *Key challenges and prospects for large wind turbines*, Renew. Sustain. Energy Rev., vol. 53, pp. 1212–1221 (2016), DOI: 10.1016/j.rser.2015.09.080.

[7] Gertmar L., Liljestrand L., Lendenmann H., *Wind Energy Powers-That-Be Successor Generation in Globalization*, IEEE Trans. Energy Convers., vol. 22, no. 1, pp. 13–28 (2007), DOI: 10.1109/TEC.2006.889601.

[8] Song Y., Wang X., Blaabjerg F., *Doubly Fed Induction Generator System Resonance Active Damping Through Stator Virtual Impedance*, IEEE Trans. Ind. Electron., vol. 64, no. 1, pp. 125–137 (2017), DOI: 10.1109/TIE.2016.2599141.

[9] Morawiec M., Blecharz K., Lewicki A., *Sensorless Rotor Position Estimation of Doubly Fed Induction Generator Based on Backstepping Technique*, IEEE Trans. Ind. Electron., vol. 67, no. 7, pp. 5889–5899 (2020), DOI: 10.1109/TIE.2019.2955403.

[10] Szypulski M., Iwański G., *Synchronization of state-feedback-controlled doubly fed induction generator with the grid*, Bull. Pol. Acad. Sci. Tech. Sci., vol. 66, no. 5 (2018), DOI: 10.24425/125334.

[11] Maciejewski P., Iwański G., *Six-phase doubly fed induction machine-based standalone DC voltage generator*, Bull. Pol. Acad. Sci. Tech. Sci., vol. vol. 69, no. 1, p. 135839 (2021), DOI: 10.24425/BPASTS.2021.135839.

[12] Gorginpour H., Oraee H., McMahon R.A., *A Novel Modeling Approach for Design Studies of Brushless Doubly Fed Induction Generator Based on Magnetic Equivalent Circuit*, IEEE Trans. Energy Convers., vol. 28, no. 4, pp. 902–912 (2013), DOI: 10.1109/TEC.2013.2278486.

[13] Torkaman H., Keyhani A., *A review of design consideration for Doubly Fed Induction Generator based wind energy system*, Electr. Power Syst. Res., vol. 160, pp. 128–141 (2018), DOI: 10.1016/j.epsr.2018.02.012.

[14] https://www.ansys.com/products/electronics/ansys-maxwell, accessed February 2022.